Applied Energy 266 (2020) 114822

Contents lists available at ScienceDirect

Applied Energy

journal homepage: www.elsevier.com/locate/apenergy

Impact of adjustment strategies on building design process in different climates oriented by multiple performance

Ran Wang[a,b], Shilei Lu[a,b,*], Wei Feng[b]

[a] School of Environment Science and Engineering, Tianjin University, 92 Weijin Road, Tianjin, 300072, China
[b] Lawrence Berkeley National Laboratory, Berkeley, CA 94720, USA

HIGHLIGHTS

- The effect of the adjustment strategy on the building design process is analyzed.
- Uncertainty analysis, sensitivity analysis, performance optimization are involved.
- Shading, window ventilation, and dimming are considered in the adjustment strategy.
- Energy, thermal and visual comfort are included in building performance.
- Various climate zones in China are compared given the impact of climate.

ARTICLE INFO

Keywords:
Uncertainty analysis
Sensitivity analysis
Optimization
Building performance
Natural ventilation
Shading and daylighting systems

ABSTRACT

Adjustment strategies including window ventilation and shading have important improvements in energy consumption, thermal and light environments, furthermore, the upper limit for improvement is affected by design parameters. However, studies incorporating adjustment strategies in the building design process are very limited. To address this research gap, we explore the effects of window ventilation and shading on building design performance from uncertainty analysis, sensitivity analysis, and multi-objective optimization. Furthermore, China's typical climate zones are compared given climate effects. Results indicate that (1) the uncertainty of total energy demand in the severe cold climate is most affected with the uncertainty increase rate being 32.0%, the uncertainty of thermal comfort ratio in the hot summer and cold winter climate and the hot summer and warm winter climate is most affected with the uncertainty increase rate being 16.3% and 14.0%, respectively. (2) the sensitivity analysis of the thermal comfort ratio is more sensitive to adjustment strategies than to total energy demand. The severe cold climate is more vulnerable than in other climates. (3) when multi-objective optimization is performed with maximum thermal comfort and minimum total energy demand when considering adjustment strategies, the severe cold climate has the greatest energy-saving potential (38.1%) and the hot summer and cold winter climate has the largest potential to improve thermal comfort (17.6%). More importantly, the light environment is within the comfort range from the daylight glare index, the illuminance, and illuminance uniformity ratios.

1. Introduction

Buildings account for about 40% of global energy consumption and more than 30% of carbon dioxide emissions [1]. The building design process is of wide concern, as most decisions about building sustainability are made at this stage [2]. This is currently highlighted in numerous high-performance building guidelines [3].

Many scholars have researched building design process, including uncertainty assessment of building performance, sensitivity analysis of design parameters, and building performance optimization. *Uncertainty assessment* refers to analyzing the uncertain distribution of building performance under the influence of various uncertain factors [4]. *Sensitivity analysis* can be used to identify the important factors affecting building performance [5]. *Building performance optimization* refers to establishing an optimization model between building design parameters and building performance (such as building energy, indoor thermal comfort), obtaining optimal design solutions using optimization methods [6]. The independent variables involved in these three

* Corresponding author.
E-mail address: lvshilei@tju.edu.cn (S. Lu).

https://doi.org/10.1016/j.apenergy.2020.114822
Received 4 November 2019; Received in revised form 6 March 2020; Accepted 7 March 2020

Nomenclature

Abbreviation

CEUI	Annual cooling energy demand [kWh/(m^{2}a)]
HEUI	Annual heating energy demand [kWh/(m^{2}a)]
LEUI	Annual lighting energy demand [kWh/(m^{2}a)]
EUI	Annual total energy demand [kWh/(m2a)]
CTR	Annual thermal comfort ratio [%]
DCTR	Annual thermal discomfort ratio [%]
SC	Severe cold climate
C	Cold climate
HSCW	Hot summer and cold winter climate
HSWW	Hot summer and warm winter climate
M	Moderate climate
TC	Thermal comfort
DS	Design scenario
NV	Natural ventilation by opening window
AS	Adjustment strategies
DGI	Daylight glare index
ISV	Illuminance standard value
DI	Daylight illuminances [lux]
WU	Wall U-value [W/(m^{2}K)]
WSH	Wall specific heat [J/(kg·K)]
SA	Solar absorptance of wall coating
WWU	Window U-value [W/(m^{2}K)]
SHGC	Solar heat gain coefficient
VLT	Window visible light transmittance
ACH	Air change rate [hr]
OA	Orientation [°]
WWR	Window-wall ratio [%]
OD	South overhang depth [m]
FD	West fin depth [m]
υ	The coefficient of variation
μ	The mean value
σ	The standard deviation
IUR	The illuminance uniformity ratios
PRCC	Partial rank correlation coefficient
MD	The maximum depth of trees
N	The number of trees
MF	The maximum of features
ESR	The energy-saving potential
CIR	The improvement rate of thermal comfort
NMBE	The standard mean deviation [%]
CVRMSE	The coefficient of variation of root mean square error [%]

Method

ANN	Artificial neural network algorithm
SVR	Support vector regression
GBDT	Gradient boosted decision trees
NSGA-II	Non-dominated sorting genetic algorithms

Subscript

s	South
w	West

types of research are steady-state design parameters, such as the building orientation, wall thermal resistance, wall specific heat, window U-value and solar heat gain coefficient (SHGC) [3].

Generally speaking, the main factors affecting building performance can be divided into two types: building design parameters (steady-state) and adjustment strategies (dynamic) [7]. Building design parameters are determined during the building design stage. Adjustment strategies (AS) are closely related to occupant behavior in the building operation stage. Although these adjustment behaviors are unknown at the building design process, research on occupant behaviors shows that occupants generally adjust the shading device and open the window according to self-comfort [8]. Through long-term field surveys in various regions, many studies have revealed some shared behavior patterns. For example, seasonal changes in window-opening behavior: the window-opening frequency was higher in non-heating seasons, especially in the transition season [9]. More important, outdoor and indoor air temperatures directly link to an occupants' window adjustment decision [10]. Rijal et al. formulated an adaptive algorithm to predict window opening using logistic regression [11]. Some adaptive thermal comfort models can be used to predict occupants' window opening behavior, based on indoor and outdoor air temperatures [12]. Fiorentini et al. applied adaptive thermal comfort criteria to windows opening in a controller, and its performance was tested via simulations and experiments [13]. For shading, internal blinds are the focus of a majority of studies, because they largely allow occupant responses through manual adjustment [14]. Occupant preference is to avoid visual discomfort with a minimum number of interactions with lighting and blind, and little consideration is paid to the exploitation of daylight dynamically, to offset electric lighting. In general, ensuring the indoor illuminance levels and avoiding glare are prerequisites for optimization analysis of shading control [15].

The impact of AS on the building design process is noteworthy because there is an interaction between AS and design parameters. The upper limit of the effect of shading and window ventilation on building performance is influenced by design parameters. For example, the window ventilation effect is the product of a complex interaction of personal behavior, building design parameters, and the outdoor environment. Its effect is all strongly related to some controllable design parameters, such as window configuration and the window to wall ratio (WWR) [16]. When a larger WWR is set up for greater ventilation, it will lead to extra heat gain through external windows and increase cooling energy demand [17]. Building orientation is also a major factor, the ventilation effect is better when the orientation of the outer window aligns with the dominant wind direction [18]. In turn, the AS also affects the optimal design parameters by changing the original heat transfer structure of building envelopes. For example, shading will change the heat exchange through the external glazing, thereby affecting the choice of SHGC. The demand for SHGC in winter and summer is reversed, which is bound to involve trade-offs. However, when using shading measures in the summer, the external window can adopt glass with a higher SHGC to get more heat gain in the winter [19]. In other words, the robustness of building performance related to operation strategies is often disregarded. A building design scheme that is optimal for one profile of determined design scenarios is not necessarily the optimal solution for most sets of occupants [20].

Only a few studies have discussed the impact of AS on building design process. For example, Chen et al. compared the preferable design solutions of a prototype high-rise residential building under design scenarios of single-sided ventilation and cross-ventilation. Optimization variables include the building layout, envelope thermophysics, building geometry, infiltration, and air-tightness [21]. Based on an office building model in a hot-dry climate, Singh et al. performed uncertainty and sensitivity analyses of energy and visual performance under the influence of external venetian blind shading. Results indicated a large uncertainty in lighting (45%), HVAC (33%) and useful daylight illuminance (106%) [22]. Rouleau et al. quantified the impacts of occupant behavior including opening windows on the residential building performance include energy consumption and comfort. Results show the

AS caused great uncertainty in building performance with a coefficient of variation of about 50% [23].

A systematic analysis of the effects of shading and window ventilation on the building design process is seldom addressed by existing research. To bridge this research gap, we identified several AS modes based on the prior probability, then analyzed their impact on the building design process including uncertainty analysis, sensitivity analysis, and building performance optimization. Furthermore, the results of four typical climate regions in China are compared considering climate differences. This research has important reference significance for robust building design.

2. Literature review

The literature review is mainly focused on methods in building design process, including (1) uncertainty analysis, (2) sensitivity analysis, and (3) building performance optimization.

2.1. Uncertainty analysis method

Because it is intuitive and easy to implement compared to other approaches, Monte Carlo analysis is a commonly used technique for uncertainty analysis [4]. Monte Carlo analysis includes three important parts: (1) specify distributions of the input variables, (2) select the sampling algorithm, and (3) create and run building performance models. In building design, the uniform distribution is commonly used in presenting possible changes in various design parameters [24]. The sampling algorithm is used to obtain the combinations of input variable values from probability density functions, the random sampling [25], Latin hypercube sampling (LHS) [26], and Sobol sequence [5] have been used in the building performance field. LHS is a stratified sampling method and is the most widely used sampling method as it can provide converged results with a small sampling number [27]. It is recommended that the sampling number is not less than 10 times the input variable [28]. Uncertainty analysis of building performance usually involves a large number of samples, which are usually implemented in conjunction with computer languages and simulation software. Simulation software including EnergyPlus [29], ESP-r [30], TRNSYS [31] and DOE-2 [32], has been used in uncertainty analysis of building performance. The uncertainty of building performance can be presented by the coefficient of variation, which is a good indicator to evaluate output dispersion [22].

2.2. Sensitivity analysis method

The order of influence of design parameters on building performance can be obtained utilizing sensitivity analysis [33]. Sensitivity analysis has been divided into local and global sensitivity methods. Global sensitivity is more reliable because it takes into account the interaction between input factors [34]. The main global sensitivity analyses are the regression method [5], the Morris method [35] and the FAST method [36]. The regression method is a commonly used global sensitivity method due to its simplicity. The standardized rank regression coefficient (SRRC) and partial rank correlation coefficient (PRCC) is the main sensitivity indicators extracted from the regression method. The difference between the two indicators is that PRCC is more suitable for correlated inputs because it can exclude the influence of the correlation between input variables [37].

2.3. Multi-objective optimization method

The optimization method based on meta-models has been widely used in related academic research [38]. With the help of machine learning algorithms, alternative models of simulation software for each performance can be separately constructed, and participate in optimization as the fitness function of the optimization algorithm [39]. This approach can reduce calls to simulation software. The artificial neural network (ANN) and the support vector regression (SVR) are two commonly used machine learning algorithms in meta-models of building performance. For example, in a study on the passive performance optimization of new residential buildings, the ANN was used to construct meta-models of thermal comfort and total energy demand [18]. In another study of the integration optimization of energy performance for high-rise buildings, SVR was used to establish meta-models for heating, cooling and lighting energy demand [3]. These results show that the meta-model effectively improves the efficiency of the optimization

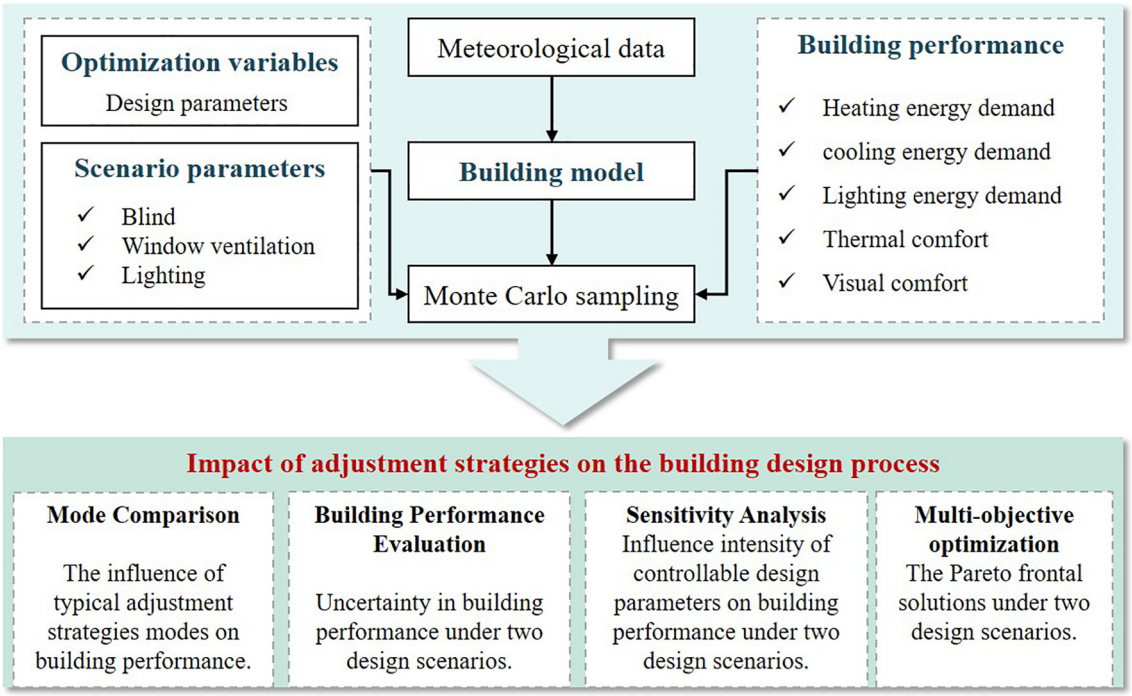

Fig. 1. The research framework.

system within the controllable accuracy range. Some studies introduce integration algorithms with higher accuracy in the field of meta-models. For example, Wang et al. applied the Gradient boosted decision trees (GBDT) algorithm to construct meta-models of building performance. The comparison with ANN and SVR highlights its superior accuracy [24].

Building performance optimization is usually a multi-scientific cross-cutting problem involving multiple performance indicators. Due to the inconsistent dimensions between each building performance, such as energy demand indicators and comfort indicators, it is difficult to integrate them into one goal [24]. For such problems, the Pareto method is a suitable choice [40]. The Pareto method can provide a set of Pareto frontal solutions, which have fewer target conflicts than other solutions. The designer can use the results to make further decisions according to their preferences [41]. Genetic algorithms belong to the group of evolutionary algorithms that can handle both continuous and discrete variables, and it has good robustness for handling complex and multivariate problems [42]. Therefore, Genetic algorithms, especially non-dominated sorting genetic algorithms (NSGA-II), are widely and effectively applied to building optimization problems [43].

3. Methodology

The research framework is composed of four phases: (1) comparison of AS modes, (2) uncertainty analysis, (3) sensitivity analysis, and (4) multi-criteria optimization. The research framework is provided in Fig. 1.

3.1. Building modelling

3.1.1. The simulation tool

A common feature of research in the building design process is the adoption of simulation software to obtain building performance data [42]. For example, Pilechiha et al. focus on the trade-offs of window design on the quality of views, daylight and building energy loads in an office room [44]. Wate et al. presented a framework for the quantification and decomposition of uncertainties in a dynamic building performance (heating and cooling load) simulation of a hypothetical office building [45]. Najjar et al. proposed an optimization framework for sustainable building by integrating a building modeling and life cycle assessment [46]. A case study with an open space office, Echenagucia et al. worked to optimize the building envelope configuration to minimize energy demand, including heating, cooling, and lighting [47]. These studies focused on all design parameters that have a potential impact on building performance, therefore, it appears that the reliability of the simulation results can be guaranteed without the need for special verification.

EnergyPlus is a very effective building simulation software that has been accepted widely by the building energy analysis community [48]. The software can be applied well to features in this study, such as shading and lighting control, window ventilation and dynamic building performance simulation. For example, Singh et al. analyzed the effects of an internal woven roller shade and glazing on energy and daylighting of an office [49]. Ascione et al. used EnergyPlus and Matlab constructed a multi-objective optimization framework for building design, considering building energy, comfort and environmental characteristics [50]. A co-simulation using EnergyPlus and Python was implemented to analyze the potential of natural ventilation for energy-savings and improved comfort [51]. EnergyPlus uses the split flux method to calculate daylight, and external illuminance in EnergyPlus is estimated using the same sky model that is used in the Daysim/Radiance programs [52]. Besides, the shading and lighting model, the airflow network module and the HVAC systems were designed to explore the maximum energy saving potential by passive measures.

3.1.2. The building model

An office in a high-rise building is selected as the case for simulation analysis. As shown in Fig. 2, the case office is located in the southwest direction. The west and south faces connect with the outside environment, and the rest sides are in contact with the air conditioning environment. The internal surface can be treated as a thermal insulation surface. Fig. 3 shows its isometric view (3.85 m × 5.90 m × 4.20 m). The window sill height is 0.75 m, and the interior surface reflectance of the floor, walls, and ceilings are 0.3, 0.5 and 0.8, respectively [53]. The internal heat gain is through lighting, office equipment, and the occupants. The occupant density in the space is 0.05 person per square meter (office hours are from 8:00 am to 6:00 pm on weekdays), and the sensible heat gain from each occupant is 76.0 W. The equipment load and the lighting power density are 7.6 W/m^2 and 11.8 W/m^2, respectively [49].

3.1.3. Integrated model

The integrated model mainly involves window ventilation, shading, and dimming. Different scenarios of occupant behavior about window ventilation are associated with the thermal sensation. Three different scenarios of occupant behavior on the opening window were modeled:

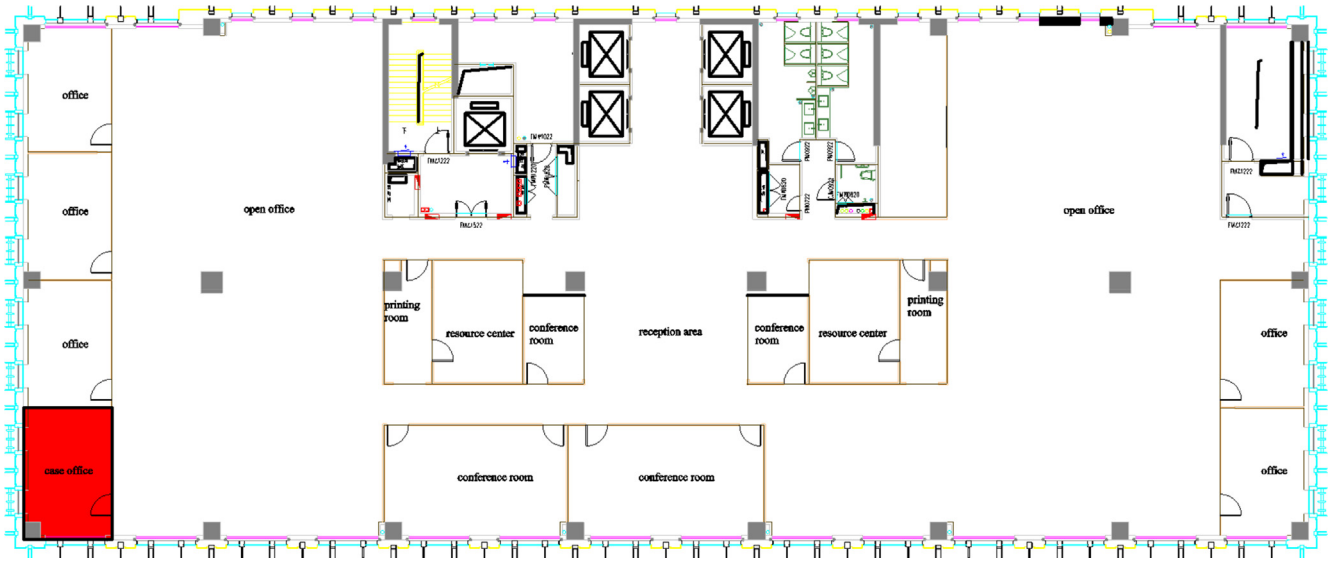

Fig. 2. The location on the floor of the case study.

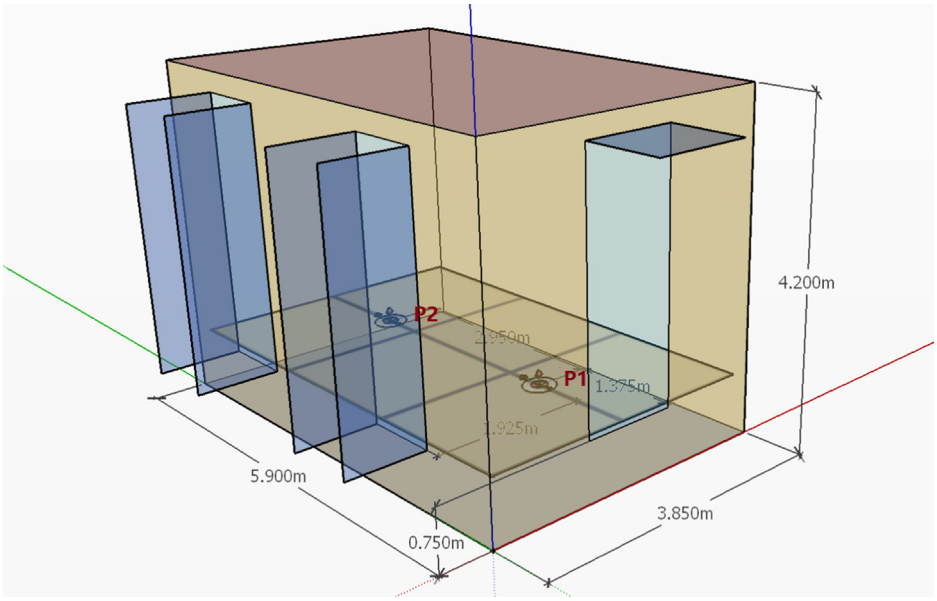

Fig. 3. Simulation model of the case office with positions of window and daylight photosensors.

(1) all-day ventilation, (2) night ventilation, and (3) adaptive adjustment. This criterion of all-day ventilation allows for window open when the external temperature is above 21 °C ($T_{ext} \geq T_{setpoint}$) when the venting availability schedule allows it. Night ventilation refers to the window open only at night when the external temperature is above 21 °C ($T_{ext} \geq T_{setpoint}$) and the venting availability schedule allows it [54]. Occupant behavior of these two scenarios is considered to be independent of the indoor temperature, as windows are always open during this time. The adaptive adjustment scenario involves window adjustment according to an adaptive thermal comfort model. The scenario allows the window open when the indoor operating temperature deviates from the thermal comfort zone and as the venting availability schedule allows it. The adaptive thermal comfort model adopted in this paper is the ASHRAE-55 model.

The comfort of the indoor light environment can be maintained by the integration of lighting and daylighting controlled by the shading device. The lighting is controlled through the two-zoned automatic dimmer, supplementing daylighting at the working plane (0.75 m from the floor). The illuminance can be measured at two control points (P1 and P2 in Fig. 3), which correspond to the center of each lighting zone. Each window is equipped with an interior blind device, and the blinds are controlled based on the glare. If the window is in a daylight zone, and if the zone's daylight glare index (DGI) exceeds the threshold specified in the daylighting object referenced by the zone, then the blinds are used. For blinds with "Block Beam Solar", the slat angle is set at each time step to just block beam solar radiation. This adjustment prevents beam solar from entering the window and causing possible unwanted glare, if the beam falls on work surfaces, while simultaneously, allowing near-optimal indirect radiation for daylighting.

The integrated modeling of shading, lighting, and window ventilation can be performed using "WindowShadingControl," "DaylightingControls" and "AirFlowNetwork" in the EnergyPlus. The flowchart of the complete procedure is presented in Fig. 4. Simulations have a time step duration of 10 min, and the availability statuses are shown in Table 1.

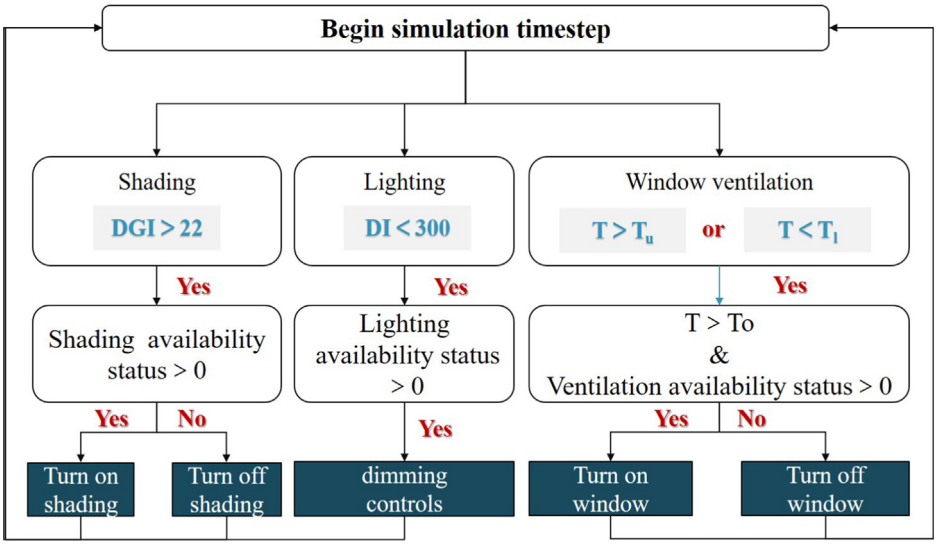

Fig. 4. The integrated model flow chart.

Table 1
The availability statuses of shading and window ventilation.

Item	Mode	Heating period	Transition season	Cooling period
Window open	1	no	no	no
	2	no	all-day	no
	3	no	all-day	night
	4	no	night	no
	5	no	night	night
	6	no	no	night
	7	no	adaptive	no
	8	no	adaptive	night
Shading	1	yes	no	no
	2	yes	no	yes
	3	yes	yes	no
	4	yes	yes	yes
	5	no	no	no
	6	no	no	yes
	7	no	yes	no
	8	no	yes	yes

3.2. Building performances

3.2.1. Visual comfort performance

When considering the integration of daylighting and lighting, visual comfort is generally evaluated in terms of light illuminance and daylight glare [55]. To ensure visual safety and efficacy during work time, the illuminance of reference planes should meet the threshold–the illuminance standard value (ISV). Based on existing reports and literature, the daylight illuminance (DI) is considered to be effective either as the sole source (300–3000 lx) or coordinated with lighting (100–300 lx) [56]. According to the GB 50034–2013 code, the ISV for offices is 300 lx and the reference plane is 0.75 m horizontally. Besides, the daylighting available at the work plane should be glare-free. The DGI is used to represent the glare intensity of daylighting because it is the most widely accepted index in the literature [49]. According to the traditional Hopkinson scale, the recommended value of maximum allowable DGI for offices is 22 [57].

The calculation for the DGI is based on [58]:

$$DGI = 10 \cdot \log\left(0.478 \sum_i \frac{L_{s,i}^{1.6} \cdot \omega_{s,i}^{0.8}}{L_b + 0.07 \cdot \omega_{s,i}^{0.5} \cdot L_{s,i}}\right) \quad (1)$$

where L_s represents the source luminance [cd/m^2], L_b represents the background mean luminance [cd/m^2], and ω_s represents the solid angle of the source [sr].

3.2.2. Thermal comfort performance

The ASHRAE-55 model is a typical adaptive thermal comfort model, designed for the indoor comfort assessment in natural ventilation conditions. The model is obtained by the analysis of 21,000 sets of data from field studies in 160 buildings worldwide and different climate zones [59]. In this paper, the ASHRAE-55 model is used to evaluate indoor thermal comfort during the transition season.

According to the ASHRAE-55 model, there is a correlation between the indoor neutral temperature (T_n) and the corresponding monthly mean outdoor temperature (T_o).

$$T_n = 0.31 \times T_o + 17.8;\ 10\ ^\circ\text{C} \leqslant T_o \leqslant 30\ ^\circ\text{C} \quad (2)$$

Considering 80% acceptability, thermal comfort fluctuates within 3.5 °C on either side of the neutral temperature (7 °C bandwidth). The upper and lower limits (T_u and T_l) are calculated based on Eqs. (3) and (4). Fig. 5 shows the thermal comfort zone of typical cities.

$$T_u = 0.31 \times T_o + 21.3 \quad (3)$$

$$T_l = 0.31 \times T_o + 14.3 \quad (4)$$

The annual thermal comfort ratio (CTR, %) can be used as the thermal comfort measure. The formula is as follows:

$$CTR = \sum_{i=1}^{q} \frac{wf_i}{q} \times 100\backslash\% \quad (5)$$

$$wf_i = \begin{cases} 1, if\ T_l \leqslant T \leqslant T_u \\ 0, if\ T < T_l or > T_u \end{cases} \quad (6)$$

where T is the indoor operating temperature, and q represents the total hour.

The indoor thermal environment is usually kept comfortable during the heating and cooling period. According to Chinese living habits, buildings are free-running during the transition season, the change of CTR mainly depends on the adjustment effect of optimization variables on the indoor thermal environment in the transition season. Therefore, the ideal value for CTR is determined by the maximum improvement achieved by adjusting design parameters, the lower limit of the CTR is determined by the minimal improvement achieved by adjusting design parameters. The CTR ranges are different in each city because the difference in climate results in different improvements achieved by adjusting design parameters. And that will be present in the result section.

3.2.3. Energy performance

Building energy performance covers all building energy demands that are highly relevant to the outdoor environment, including annual heating, cooling, and lighting energy demands.

The calculation of energy demand is obtained by using Eqs. (7)–(9):

$$HEUI = \sum_{i=1}^{i=m} EU_{hi}/M \quad (7)$$

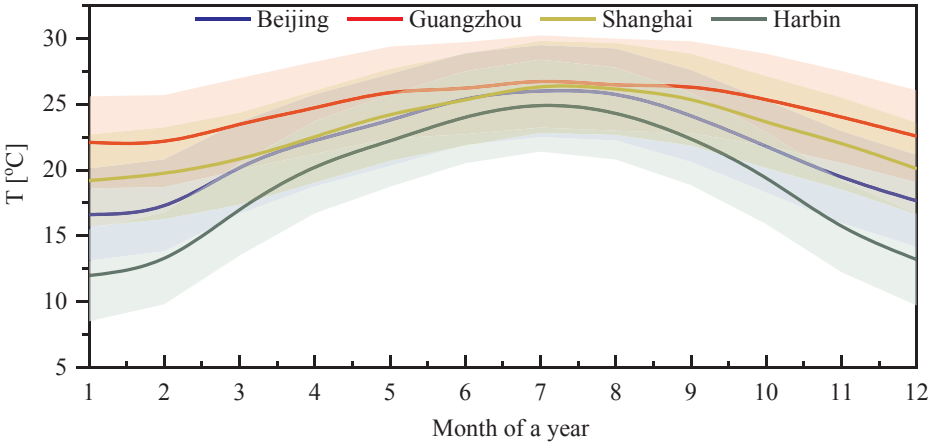

Fig. 5. The thermal comfort zone of typical cities.

$$CEUI = \sum_{i=1}^{i=n} EU_{ci}/M \tag{8}$$

$$LEUI = \sum_{i=1}^{i=h} EU_{li}/M \tag{9}$$

$$EUI = HEUI + CEUI + LEUI \tag{10}$$

Among them, the m, n and h represent the cumulative hours of annual required heating, cooling, and lighting, respectively. The *HEUI*, *CEUI,* and *LEUI* represent the annual heating, cooling, and lighting energy demands in kWh/(m^2a). The EUI is the total building energy demand in kWh/(m^2a). The EU_{hi}, $EU_{ci,}$ and EU_{li} represent the heating load, cooling load and lighting power load of the total space in kW/m^2. The M represents the space area in m^2.

3.3. Design parameters

The optimization variables involved are mainly passive design parameters, including the wall U-value (WU), the wall specific heat (SH), the solar absorptance of wall coating (SA), the window U-value in the south and west (WWU_s and WWU_w), the solar heat gain coefficient in the south and west ($SHGC_s$ and $SHGC_w$), the window visible light transmittance in the south and west (VLT_s and VLT_w), air change rate (ACH), orientation (OA), WWR in the south and west (WWR_s and WWR_w), south overhang depth (OD) and west fin depth (FD). These variables are potentially influential in building performance, according to existing literature.

All variables are continuous with the boundary covering the actual material properties. The wall is addressed with a combination of variable SH and WU as well as fixed wall dimensions and densities in the EnergyPlus model. This combination can represent the thermal characteristics of existing wall structures [60]. The ACH complies with the building code of China and the European Union [61]. The range of VTL and SHGC can cover existing exterior window products, from ordinary exterior windows to three-layer low-E (low emissivity)windows [62]. The SA of the wall coating covers the color value from shallow to deep [18]. The distribution form and range of these design parameters are shown in Table 2.

3.4. Statistical method

3.4.1. The sensitivity analysis

The PRCC extracted from the regression method can be used as a sensitive indicator. For input, X $= x_{ij}\ldots, I = 1, \ldots, n; j = 1,\ldots, m$. The n and m represent the sample size and the number of input variables, respectively.

The regression method' form is shown in Eq. (11):

$$y_i = b_o + \sum_j b_j x_{ij} + \varepsilon_i \tag{11}$$

where y_i is the output, and ε_i is the residual due to the approximation. The coefficient b_j is determined by the least square method.

The correlation coefficient (CC) between x and y is shown in Eq. (12).

$$CC = r_{xjy} = \frac{Cov(x_j, y)}{\sqrt{Var(x_j)Var(y)}} = \frac{\sum_{i=1}^{n}(x_{ij} - \bar{x})(y_i - \bar{y})}{\sqrt{\sum_{i=1}^{n}(x_{ij} - \bar{x})^2}\sqrt{\sum_{i=1}^{n}(y_{ij} - \bar{y})^2}} \tag{12}$$

PCC is calculated according to Eq. (13).

$$\begin{aligned} PCC &= CC((Y - \hat{Y}), (X_j - \hat{X}_j)) \\ \hat{Y} &= b_o + \sum_{h\neq j} b_h x_h \\ \hat{X} &= c_o + \sum_{h\neq j} c_h x_h \end{aligned} \tag{13}$$

The poor linear fits can often be avoided with the use of rank transformations, which involves replacing the data with their corresponding ranks. Then, the usual least squares regression analysis is performed entirely on these ranks. The PRCC is obtained after rank transformation.

3.4.2. The uncertainty analysis

LHS can be used to extract a representative sample set of input variables. The coefficient of variation (υ) is used to evaluate the uncertainty of building performance indicators.

The calculation of υ is as follows:

$$\upsilon = \sigma/\mu \tag{14}$$

$$\mu = \frac{1}{n}\sum_{i=1}^{n} y_i \tag{15}$$

$$\sigma = \sqrt{\frac{1}{n-1}\sum_{i=1}^{n}(y_i - \mu)^2} \tag{16}$$

Among them, "μ" and "σ" are the mean value and the standard deviation, respectively. "n" represents the sample size. "y" is the output of each sample.

3.5. Optimization model

An important intent of this paper is to study the impact of AS on the optimal design scheme. The established optimization model is multi-dimensional, intending to minimize the total building energy demand and maximize the dynamic thermal comfort ratio. The optimization variables are design parameters, defined in Section 3.3. In addition, the optimization model is constrained by design parameter boundaries and visual comfort.

The optimization function (*OF*) is defined as Eqs. (17) and (18).

$$OF = \begin{bmatrix} f_1 = f(\vec{x}, HEUI)_{\min} \\ f_2 = f(\vec{x}, CEUI)_{\min} \\ f_3 = f(\vec{x}, LEUI)_{\min} \\ f_4 = f(\vec{x}, CTR)_{\max} \end{bmatrix} \tag{17}$$

Subject to

$$\begin{cases} \vec{x} = \vec{x}_{range} \\ DI = 300 \\ DGI \leqslant 22 \end{cases} \tag{18}$$

Table 2
The description and range of design parameters.

Abbreviation	Unit	Distribution form	Range
WU	W/(m^2K)	continuous uniform distribution	[0.1, 1.58]
SH	J/(kg·K)	continuous uniform distribution	[800, 2000]
SA	/	continuous uniform distribution	[0.1, 0.9]
WWU_s	W/(m^2K)	continuous uniform distribution	[1.204, 5.912]
SHGCs	/	continuous uniform distribution	[0.102, 0.897]
VLTs	/	continuous uniform distribution	[0.035, 0.921]
WWU_w	W/(m^2K)	continuous uniform distribution	[1.204, 5.912]
$SHGC_w$	/	continuous uniform distribution	[0.102, 0.897]
VLTw	/	continuous uniform distribution	[0.035, 0.921]
ACH	hr	continuous uniform distribution	[0.5, 1.5]
OA	°	continuous uniform distribution	[0, 360]
WWR_s	/	continuous uniform distribution	[0.275, 0.730]
WWR_w	/	continuous uniform distribution	[0.308, 0.619]
OD	m	continuous uniform distribution	[0, 2]
FD	m	continuous uniform distribution	[0, 2]

3.6. Meta-based optimization method

Under comprehensive consideration, this paper adopts the GBDT-based NSGA-II as the optimization method. the GBDT, an integrated machine learning algorithm [63], is used to build meta-models. The detailed construction process of this algorithm is described in reference [64]. The main parameters affecting GBDT performance are the maximum depth of trees (MD), the number of trees (N), and the maximum of features (MF) [24]. The accuracy indicators specified in ASHRAE Guideline 14-2002 can be introduced to evaluate the performance of meta-models. When the standard mean deviation (NMBE) and the coefficient of variation of root mean square error (CVRMSE) is less than ± 5% and ± 15%, respectively, the model is accurate and eliable [65]. In the Python environment, meta-models established by GBDT can be used as the fitness function of NSGA-II to participate in the optimization process.

The calculation of NMBEand CVRMSE is as follows:

$$NMBE = \left| \frac{\sum_{i=1}^{i=n} (y_i - \hat{y}_i)}{n \times \bar{y}} \right| \times 100\% \tag{19}$$

$$CVRMSE = \frac{\sqrt{\frac{1}{n}\sum_{i=1}^{i=n} (y_i - \hat{y}_i)^2}}{\bar{y}} \times 100\% \tag{20}$$

where they_i, $\hat{y}_i$ and $\bar{y}$represents the actual value, the predicted value, and the average actual value, respectively.

3.7. Weather conditions of the major climatic zones in China

According to China's national standard GB50176-93 [66], China is divided into five major climate zones, namely severe cold (SC), cold (C), hot summer and cold winter (HSCW), hot summer and warm winter (HSWW), and moderate (M). These divisions are based on the average temperatures in the coldest and hottest months. Because the building design in the M climate generally does not consider heating and cooling demands, this study does not consider the M climate. Typical cities in the four remaining climates are selected: Harbin, Beijing, Shanghai, and Guangzhou. The climate zones and the monthly meteorological parameters of the corresponding cities are shown in Fig. 6.

4. Results and discussion

4.1. The impact of various strategy modes on building performance.

Fig. 7 shows the influence of various modes of AS on the annual thermal comfort and the annual heating/cooling/lighting energy demands. As shown in Fig. 7(a), shading, night ventilation, and their interactions, all can reduce the CEUI for the four cities. The AS has the greatest potential for cooling energy-saving in Beijing, compared to the other cities. For each city, differences in the cooling energy-saving potential of different mode AS exist. By mode 1 vs mode 3 or mode 2 vs mode 4, night ventilation does reduce the cooling load, especially when shading is not considered. However, by mode 1 vs mode 2, the influence of shading on CEUI has the opposite result, with changes in the city and the ventilation mode. When considering shading only, the cooling energy demand in Guangzhou will increase. The main reason is that shading not only affects the solar radiation heat but also the lighting power. When coupling the daylighting and lighting, closed shading will reduce the solar radiation heat while reducing the available daylighting illuminance. In the case of maintaining indoor illuminance meeting the comfort requirements, the lighting energy demand increases. Therefore, the inner heat gain caused by the heat dissipation of lighting increases, which leads to increased CEUI. This indicates that the influence of shading on CEUI will have the opposite result, depending on the solar radiation distribution and lighting power density, when using coupling daylighting and lighting. By mode 3 vs mode 4, the interaction of night ventilation and shading increases the CEUI. This is because night ventilation reduces the daily cooling load by reducing the indoor heat storage, and their total reduction is greater than the increased heat dissipation caused by lighting. In conclusion, the impact of AS on CEUI is determined by a combination of the lighting control mode, solar radiation distribution, and indoor heat storage.

As shown in Fig. 7(b), shading leads to increased HEUI during the heating season. The increase is from large to small, Harbin > Beijing > Shanghai, and it can be largely negligible for Shanghai. Fig. 7(c) shows the effect of two lighting modes (switch and continuous dimming control) on the LEUI. Since the power of switch lighting is not affected by changes in outdoor weather conditions, the LEUI in all cities is the same, at 26.3 kWh/(m^{2}a). When using continuous dimming control, daylighting is effectively utilized, and the lighting energy is saved while maintaining normal illuminance. All four cities have great energy-saving potentials with continuous dimming control, but the energy-saving potential of Shanghai is the highest.

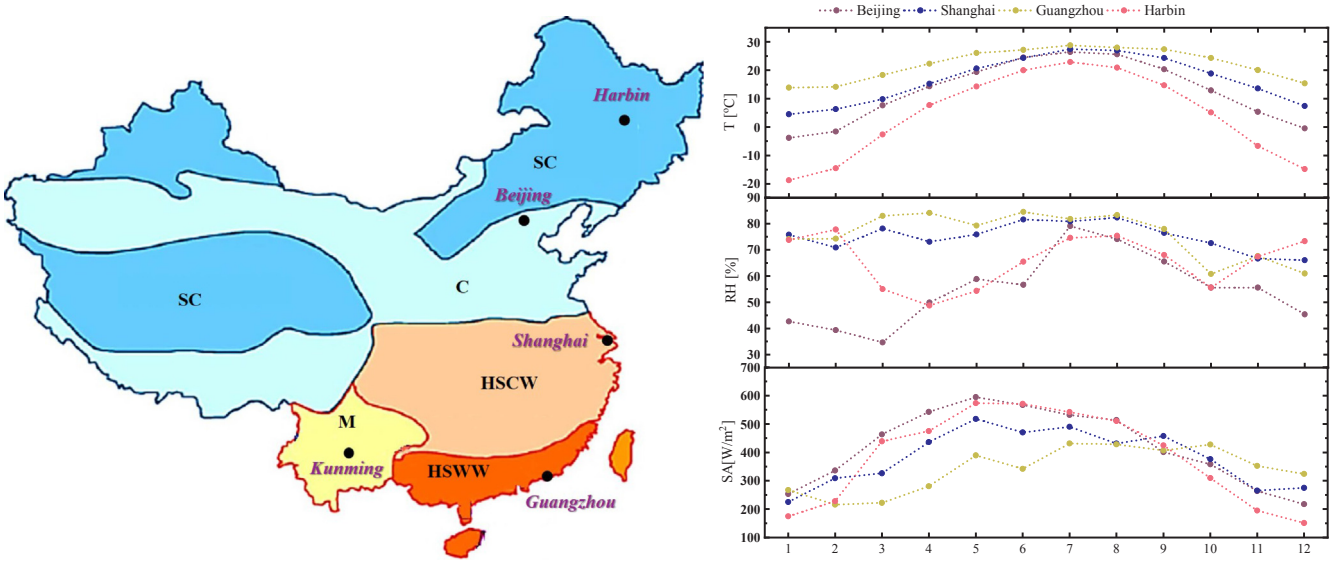

Fig. 6. Climate zones and outdoor meteorological parameters for typical cities.

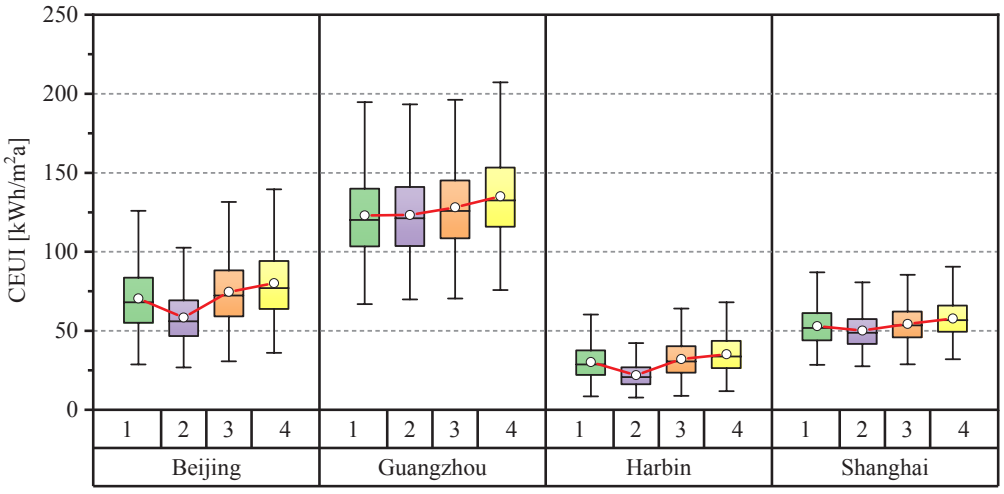

a) The cooling energy demand during the cooling season. (*Mode 1: with night NV & shading; mode 2: with night NV & without shading; mode 3: without NV & with shading; mode 4: without NV & without shading.*)

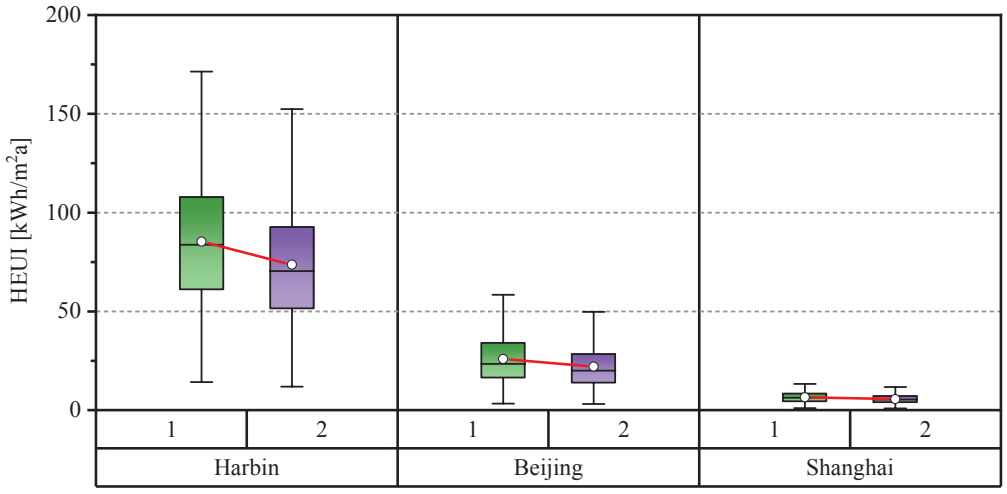

b) The heating energy demand during the heating season. *(Mode1: without NV & with shading; mode2: without NV & without shading.)*

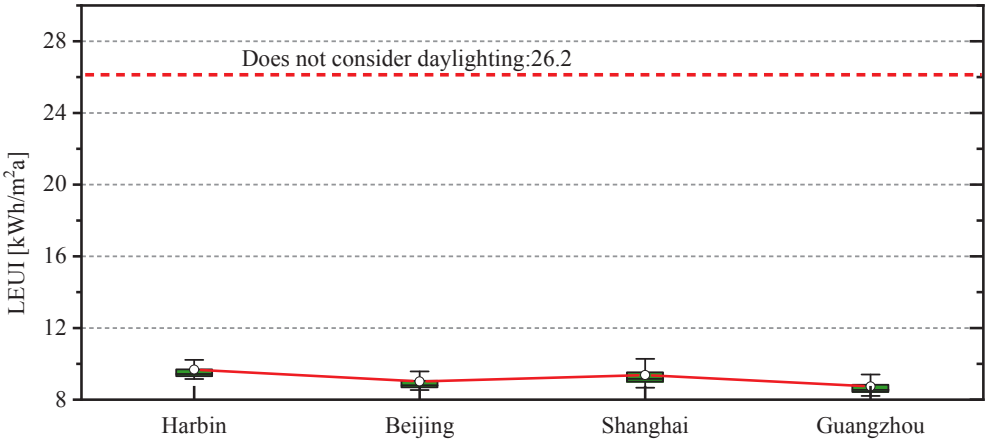

c) The lighting energy demand under integrated control of daylighting and lighting.

Fig. 7. The building performance under different AS mode.

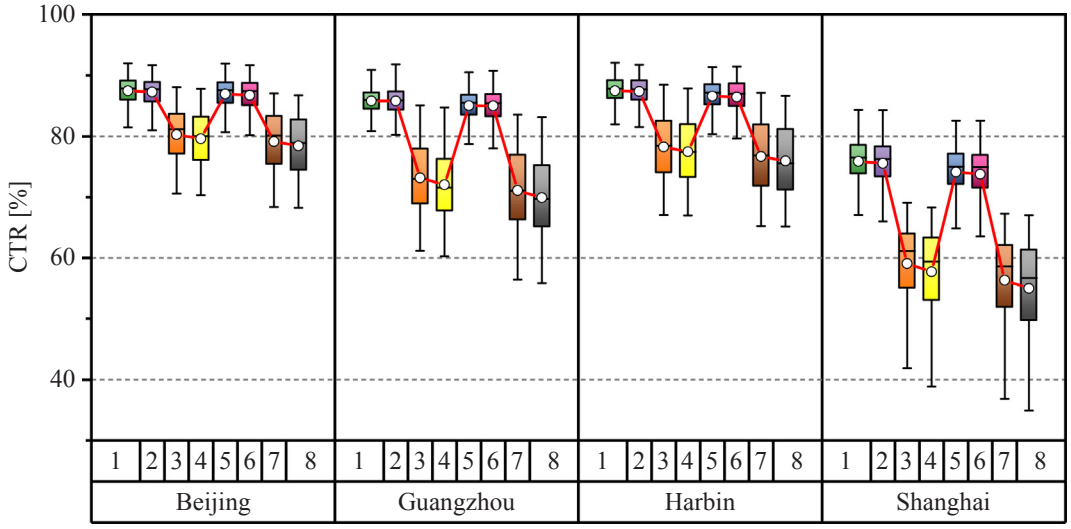

d) The annual indoor thermal comfort during transition season. *(Mode 1: all-day NV & shading; mode 2: all-day NV & without shading; mode 3: night NV & shading; mode 4: night NV & without shading; mode 5: adaptive NV & shading; mode 6: adaptive NV & without shading; mode 7: without NV & shading; mode 8: without NV & without shading.)*

Fig. 7. (*continued*)

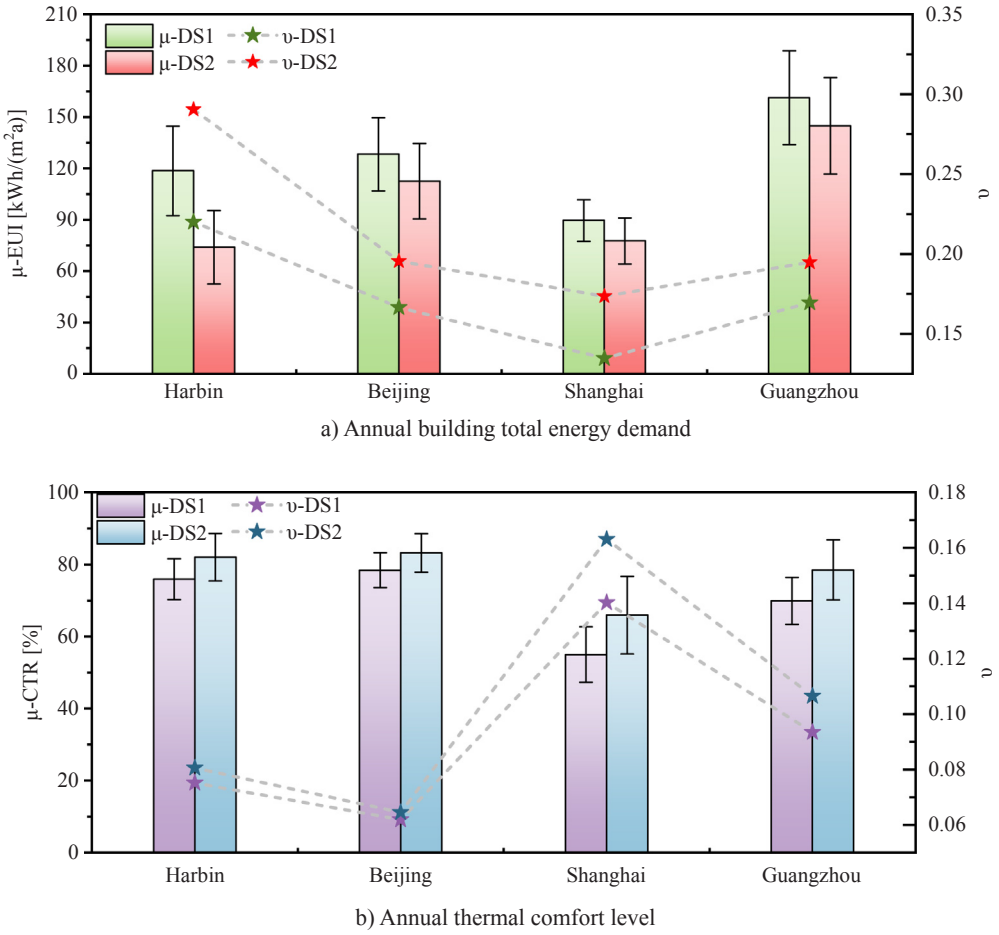

Fig. 8. Uncertainty analysis of building performance.

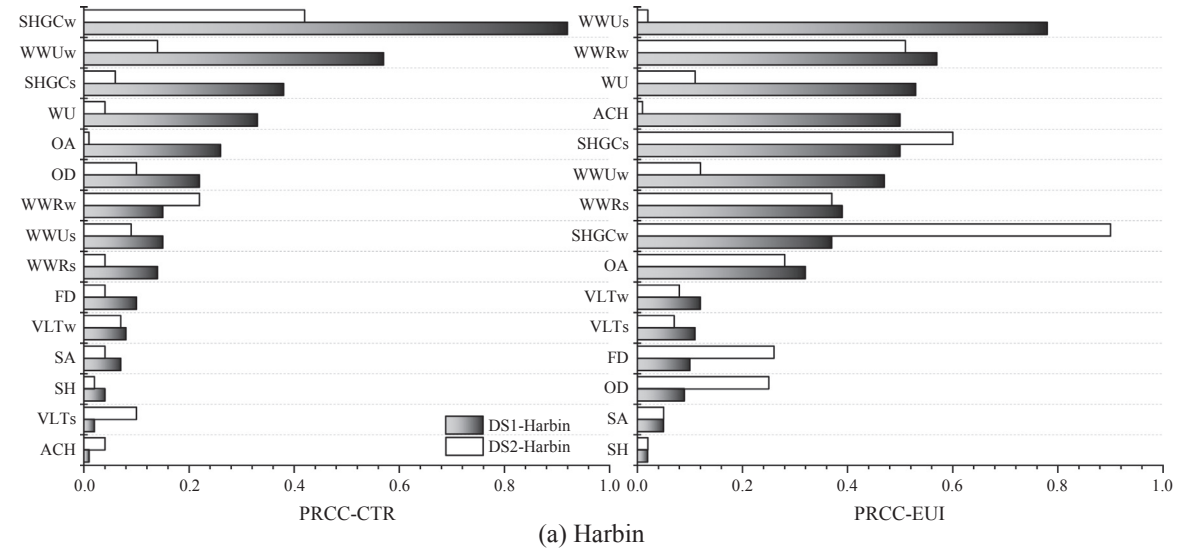

(a) Harbin

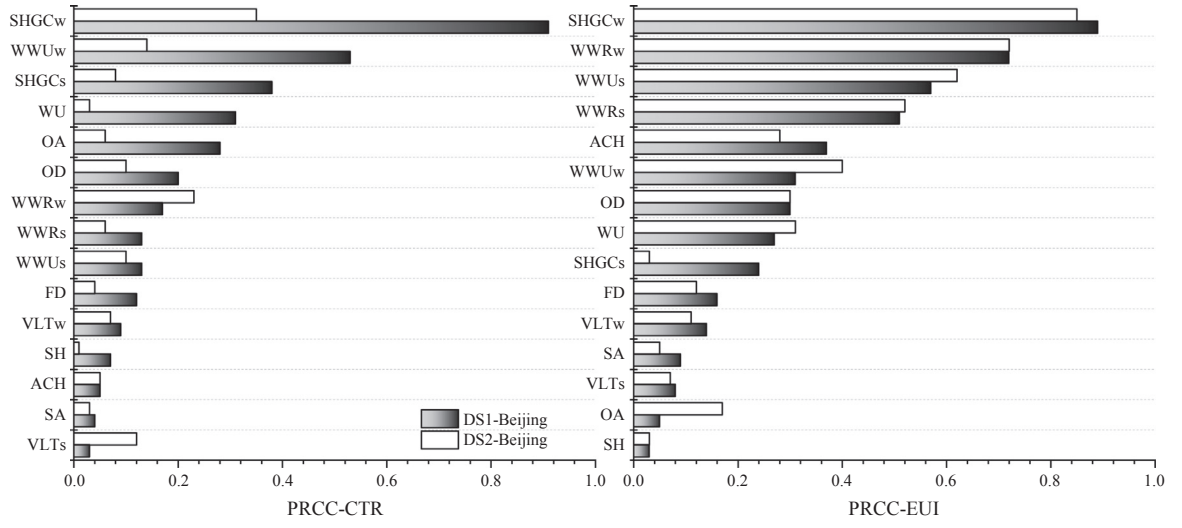

(b) Beijing

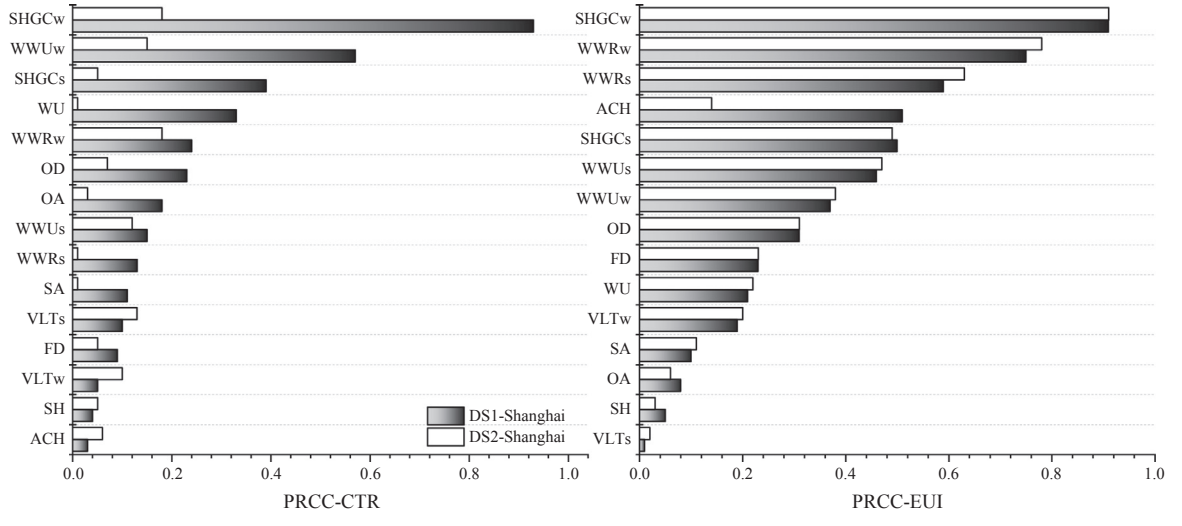

(c) Shanghai

Fig. 9. The PRCC indicator of design parameter on CTR and EUI under two design scenarios.

Fig. 7(d) shows the impact of different strategy modes on indoor thermal comfort during the transition season. When not considering AS, the overall thermal comfort level in Shanghai is the worst, and that of Beijing and Harbin is best. When considering AS, the indoor thermal comfort in Beijing, Shanghai, and Harbin are almost the same. By mode 1, mode 3 and mode 5 vs mode 7 or mode 2, mode 4, mode 6 vs mode 8, NV can significantly improve thermal comfort. In addition, by comparing modes 1 and 5 or modes 2 and 6, the influenced difference between all-day NV and adaptive NV is largely negligible. Therefore, for offices that do not allow window-opening at night, adaptive NV can be performed. The ability of night NV to improve thermal comfort is much lower than that of all-day NV and adaptive NV modes. Furthermore, the lower the basic scenario (without AS), the greater the potential for improving thermal comfort. By mode 1 vs mode 2, mode 3 vs mode 4, mode 5 vs mode 6 or mode 7 vs mode 8, the improvement of shading is largely influenced by NV modes, which is masked by the relatively large improvement potential of NV. The shading has a significant effect on thermal comfort, only when without NV or for night NV.

In summary, AS have different emphases on building performance, in different climate zones. That is, increasing HEUI in SC climates, reducing CEUI in C climates, improving the indoor thermal comfort for HSCW climates, improving the daylighting effect and reducing the LEUI for HSWW climates.

4.2. Uncertain analysis of building performances

This section explores how much AS has affected the uncertainty of early building performance assessments. Because the dimensions are consistent, the heating, cooling and lighting energy demand can be integrated into the total energy demand. Fig. 8 shows the uncertainty index of EUI and CTR in all cities. Among them, the design scenario 1 (DS1) represents not considering AS, and the design scenario 2 (DS2) represents considering AS.

Fig. 8(a) presents the μ and υ of EUI. By comparing the μ between two design scenarios, the energy-saving potential of AS is the largest in Harbin and ranks down by Guangzhou, Beijing, and Shanghai. A higher υ indicates a large dispersion of EUI. For all cities, there are large differences in the υ between the two design scenarios. This means that the AS will greatly increase the uncertainty in early building energy assessment. Compared with DS1, the uncertainty increase rate of EUI in DS2 is 32.0%, 17.3%, 28.8% and 14.8% for Harbin, Beijing, Shanghai, and Guangzhou, respectively. Therefore, the cities in descending order of impact intensity are Harbin, Shanghai, Beijing, and Guangzhou.

Fig. 8(b) presents the μ and υ of CTR. By comparing the μ between two design scenarios, the improvement potential for the thermal comfort of AS is the largest in Shanghai and then ranked by Guangzhou, Harbin, and Beijing. By comparing the υ between two design scenarios, the impact of AS on the uncertainty in CTR assessment in Harbin and Beijing is relatively small with the υ increase rate being 7.2% and 4.2%, respectively. However, the impact of AS on CTR in Shanghai and Guangzhou is relatively significant, with the υ increase rate being 16.3% and 14.0%, respectively.

4.3. Sensitivity analysis

This section explores whether the impact of each design parameter on building performance changes when considering the potential impact of AS on building performance in the design phase. The influence of each design variable on building performance indicators can be expressed by the PRCC index.

Fig. 9 shows the PRCC result in two design scenarios for each city. The PRCC of CTR is more susceptible to AS than that of EUI in all cities. Moreover, the influence intensity of most design parameters on CTR is weakened. For all cities, $SHGC_w$, $SHGC_s$, WWU_w, and WU are the most important factors with PRCC being more than 0.3. At the same time, their sensitivity is relatively affected by AS. The SH, VLT_w, VLT_s, ACH, and SA are considered relatively less important with individual contributions less than 10%. Comparing the PRCC in the two design scenarios, the impact of VLT_s on CTR is enhanced in DS 2. The main reason is that daylighting supplements lighting in this design scenario. The indirect impact of VLT on the indoor thermal environment is enhanced by affecting the shading state. The effect of AS on the PRCC results of EUI can be almost ignored except in Harbin. For Harbin, the PRCC value of WWU_s, WWR_w, WU, ACH, $SHGC_s$, and WWU_w are at the forefront. These are followed by WWR_s, $SHGC_w$, and OA. Among them, the influence intensity of WWU_s, WU, ACH, WWU_w, and $SHGC_w$ have significant differences in the two design scenarios. For the other three cities, the $SHGC_w$ is determined to be the most important contributor for EUI, and WWR_w and WWR_s are also important factors, while their ranks are slightly different in different cities. In addition, it should be mentioned that the importance of ACH to EUI has declined for all cities. Overall, CTR is more sensitive to AS than EUI. The Harbin is more vulnerable than in other areas.

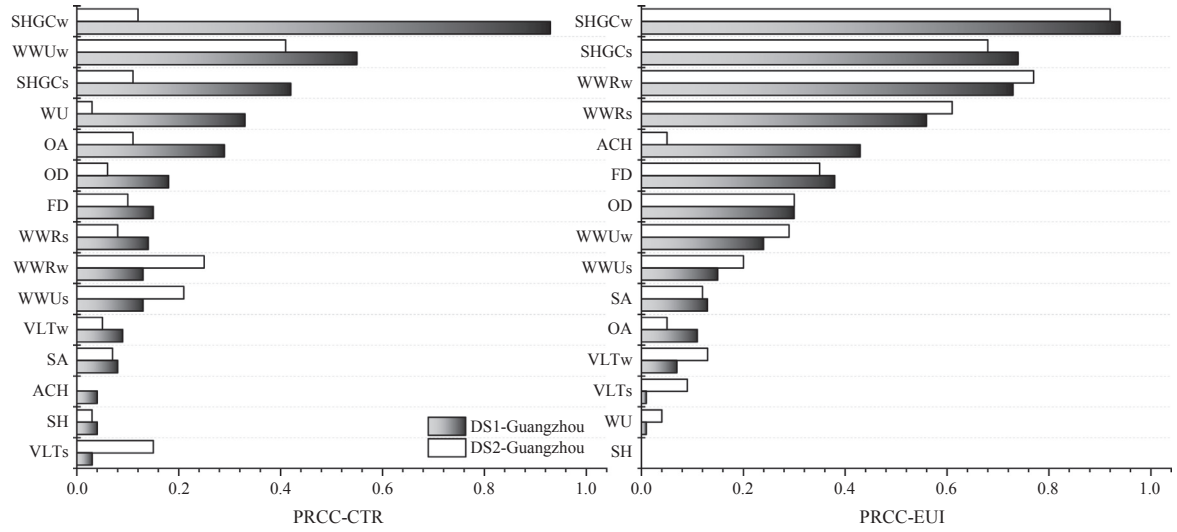

(d) Guangzhou

Fig. 9. (*continued*)

4.4. Pareto frontier solution

GBDT based NSGA-II method is run to obtain the Pareto frontier design space. The aim is to find the optimal values of the 15 design variables for maximizing the CTR while minimizing the EUI. Since the criterion of the NSGA-II algorithm is that all targets are minimized, the annual thermal discomfort ratio (DCTR) is minimized in the optimization process, instead of maximizing the CTR. Tuning hyperparameters when build meta-models using GBDT, and Table 3 shows the optimized hyperparameters. Table 4 presents the accuracy metrics of GBDT-based meta-models in four cities. All meta-models meet the requirements of ASHRAE Guideline 14-2002 with the NMBE and CVRMSE less than 5% and 15%, respectively. In terms of the NSGA-II algorithm, several important optimization settings are summarized in Table 5.

The Pareto frontier solution under two design scenarios is shown in Fig. 10. In DS 1, For Guangzhou, EUI varies from 98.9 to 106.1 kWh/(m^2a) and DCTR varies from 15.1% to 17.3%; For Shanghai, EUI varies from 61.0 to 68.0 kWh/(m^2a) and DCTR varies from 30.5% to 33.4%. For Beijing, EUI varies from 75.3 to 91.2 kWh/(m^2a) and the DCTR varies from 11.0% to 14.1%. For Harbin, EUI varies from 53.0 to 99.8 kWh/(m^2a) and DCTR varies from 11.6% to 14.7%. In DS 2, the Pareto frontier solution for four cities all move toward the direction in which the optimization goal becomes smaller. For Harbin, the AS has the greatest impact on EUI in the frontier solution, with the maximum and minimum values reducing by 54.9 and 28.2 kWh/(m^2a), respectively. For Shanghai, the AS has the greatest impact on the DCTR in the frontier solution, with the maximum and minimum values reducing by 10.5% and 15.3%, respectively.

4.5. Post optimization analysis

In the decision-making stage, indoor comfort is the most important demand from the occupant's perspective. Therefore, it is a decision-making direction for designers to priority the solution with the largest thermal comfort. On the basis of the Pareto solution, the solution that prioritizes the maximum CTR and then minimum EUI in each design scenario is shown in Fig. 11. Moreover, the energy-saving potential (ESR) and the improvement rate of thermal comfort (CIR) are also calculated and displayed. The energy-saving potential of Guangzhou reached 20.4%, and that of the other three cities reached more than 30.0%, especially Harbin (38.1%). In terms of the improvement rate of thermal comfort, Shanghai has the largest potential (17.6%), while the other three cities have less than 10% potential, especially Beijing (3.3%).

Table 6 shows the values of the design parameters corresponding to Fig. 11. For all cities, the design parameters of the optimal solution tend to a higher insulation level (i.e., WU, WWU_s, and WWU_w tend to smaller values) in DS 2. The SH tends to larger values in Harbin and Beijing but remains almost unchanged in Shanghai and Guangzhou. The value of SA tends to larger values in all the cities.

In terms of the indoor light environment, the illuminance and DGI of the two reference points P1 and P2 are shown in Fig. 12. When excluding the outliers, the DGI of the four cities is within the comfort threshold of 22. And the difference in DGI between two reference points is small. Except for point A in Shanghai, the dynamic illumination throughout the year of all reference points is maintained below 2,000 lx. Since reference point P1 accepts more south and west windows at the same time, its illuminance is higher than point P2. According to existing research, daylight illuminances in the 300–3000 lx range are often perceived either as desirable or at least tolerable [56]. In addition, human vision is more sensitive to lighting contrast in an area than to the daylighting amount. Therefore, uniformity is an important factor for visual comfort in addition to glare and illumination. This uniformity can be described through illuminance uniformity ratios (IUR), which refer to the ratio of illuminance P1 to P2. Regarding acceptable illuminance uniformity, CIBSE in 1987 recommended IUR from all sources to be less than or equal to 1:3, with supplementary lighting compensating differences from daylighting [67]. Fig. 13 shows the boxplot of IUR in each city. The illumination uniformity of the four cities all can meet the comfort requirements, with the upper quartiles of IUR being below 3.5. Overall, the indoor light environment is within the comfort range or acceptable.

Table 4
Accuracy metrics of GBDT-based meta-models.

Indicator		Harbin		Beijing		Shanghai		Guangzhou	
		DS1	DS2	DS1	DS2	DS1	DS2	DS1	DS2
CVRMSE (%)	EUI	7.54	0.75	4.75	0.75	4.04	0.47	3.72	0.38
	DCTR	5.60	0.33	5.22	0.34	3.12	0.23	4.38	0.37
NMBE (%)	EUI	2.43	0.01	1.66	0.00	0.49	0.02	0.21	0.02
	DCTR	0.11	0.02	1.73	0.01	0.21	0.01	0.39	0.01

Table 5
The setting of the NSGA-II algorithm.

Parameter	Value
Population size	50
The number of maximum generation	200
Generation gap	0.5
Crossover probability	0.7
Mutation probability	1

5. Conclusion

This paper establishes a framework to analyze the impact of adjustment strategies on the building design process. Based on the principle of occupant's comfort, the adjustment strategy model is established to integrate shading, natural ventilation, and dimming. Considering and not considering adjustment strategies are two design scenarios. Four typical climates in China are compared given their climate differences. The influence of adjustment strategy on building design process is mainly analyzed from the following four aspects: (1) the influence of different adjustment strategy modes on various aspects of building performance, including heating, cooling and lighting energy

Table 3
The optimized hyperparameters of GBDT-based meta-models.

Design scenario	Hyperparameter	Harbin		Beijing		Shanghai		Guangzhou	
		EUI	DCTR	EUI	DCTR	EUI	DCTR	EUI	DCTR
DS1	MD	10	5	7	10	5	4	5	4
	MF	9	15	15	10	15	15	15	15
	N	2000	2000	2000	2000	2000	2000	2000	2000
DS2	MD	10	10	10	10	5	10	10	10
	MF	15	15	17	17	11	15	15	10
	N	2000	1000	2000	2000	2000	1000	2000	2000

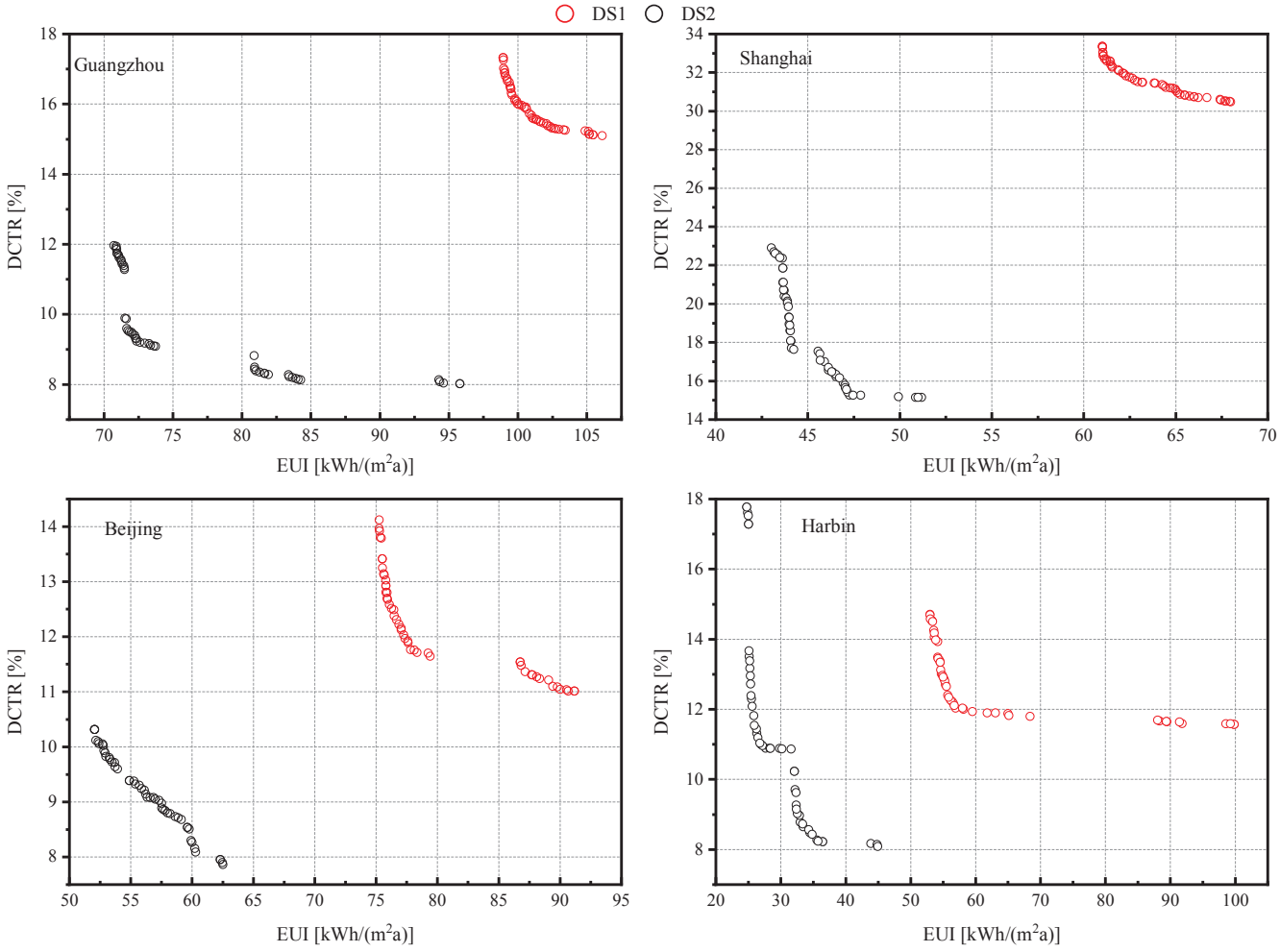

Fig. 10. The Pareto optimization results.

demand, as well as dynamic thermal comfort; (2) uncertainty analysis of total building energy demand and dynamic thermal comfort; (3) sensitivity analysis of design parameters to total building energy demand and dynamic thermal comfort; and (4) the Pareto frontier solution aims to minimize total building energy demand (including heating, cooling and lighting energy demand) and maximum thermal comfort.

The main findings are as follows:

(1) The adjustment strategy has a different influential emphasis in various climate zones, including increasing the heating energy demand in severe cold climate, reducing the cooling energy demand in cold climates, improving the indoor thermal comfort in the hot summer and cold winter climates, and reducing the lighting energy demand in the hot summer and warm winter climate. Furthermore, the effect of adjustment strategies on cooling energy demand is affected by the combination of lighting modes, solar radiation distribution, and indoor heat storage. The improvement of shading on indoor thermal comfort is largely influenced by window ventilation modes, and that is significant only in the without ventilation mode or night ventilation mode. The powerful improvement potential of adaptive ventilation and all-day ventilation masks the effect of shading. Shading will increase the heating energy demand, but the coupling of shading and dimming will avoid glare and significantly reduce the lighting energy demand.

(2) The uncertainty of total energy demand in the severe cold climate is most affected by the adjustment strategy, and the uncertainty increase rate is 32.0%, 17.3%, 28.8% and 14.8% for the severe cold, the cold, the hot summer and cold winter, as well as the hot summer and warm winter climate, respectively. The impact of adjustment strategies on annual thermal comfort ratio in the hot summer and cold winter and the hot summer and warm winter climate is relatively significant, with their uncertainty increase rates being 16.3% and 14.0%, respectively. In the cold climate and the severe cold climate, the uncertainty increase rate is relatively small, at 4.2% and 7.2%, respectively.

(3) According to the PRCC indicators, the sensitivity analysis results of the annual thermal comfort ratio are more sensitive to adjustment strategies than that of total energy demand. The severe cold climate is more vulnerable than in other climates. The influence intensity of most design parameters on the annual thermal comfort ratio is weakened under the design scenarios that consider the adjustment strategy. For all cities, SHGC for west and south windows, the U-value for the west window, and the wall U-value are the most important factors for the annual thermal comfort ratio with PRCC being more than 0.3. At the same time, their sensitivity is subject to relatively large impact strength.

(4) Adjustment strategies move the Pareto frontal solutions of all cities in a better direction. The severe cold climate and the hot summer and cold winter climate have the greatest potential to reduce total energy demand and discomfort ratios, respectively. Make further decisions on the Pareto frontal solution, when the minimum energy demand is satisfied on the basis of optimal thermal comfort, the energy-saving potential of the hot summer and warm winter climate reach 20.4%, and that of the other three cities reach more than 30.0%, especially the severe cold climate (38.1%). The hot summer and cold winter climate has the largest potential to

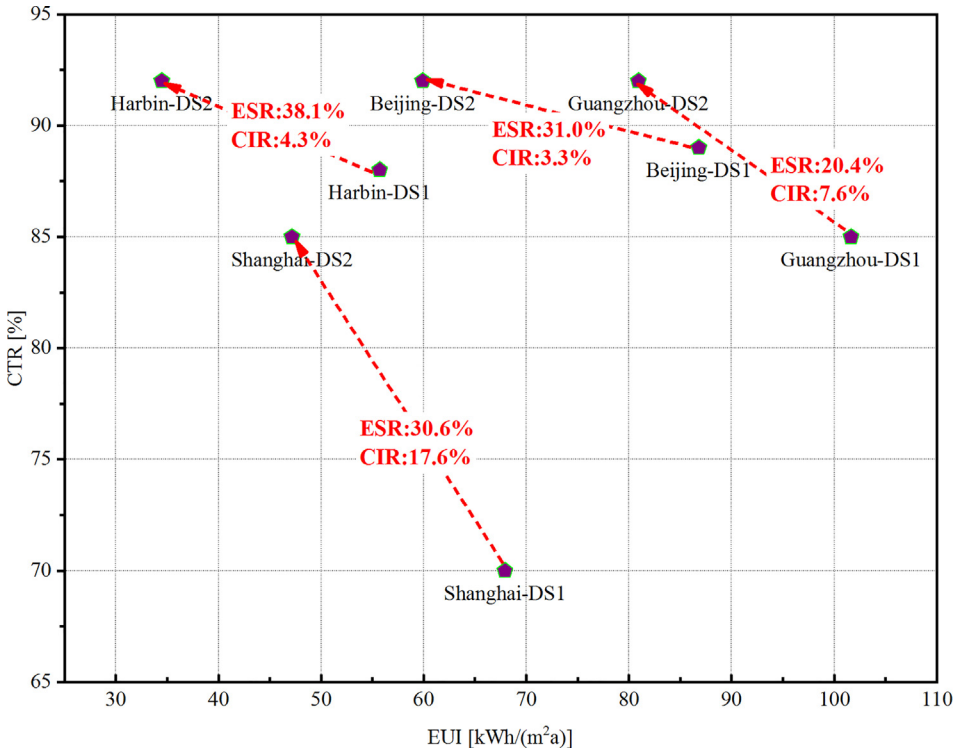

Fig. 11. Comparison of optimal solutions for two design scenarios when thermal comfort is optimal.

Table 6
The corresponding design parameters of when priority is given to optimal comfort.

Variable	Harbin-DS1	Harbin-DS2	Beijing-DS1	Beijing-DS2	Shanghai-DS1	Shanghai-DS2	Guangzhou-DS1	Guangzhou-DS2
WU	0.34	0.20	1.03	0.12	1.58	0.10	1.03	0.10
SH	830.47	1173.68	807.06	1624.55	1587.85	1593.92	854.41	862.54
SA	0.65	0.83	0.15	0.57	0.12	0.31	0.13	0.28
WWU_s	2.37	1.50	2.30	1.67	4.13	1.36	2.41	1.29
SHGCs	0.66	0.12	0.11	0.77	0.11	0.24	0.14	0.15
VLTs	0.66	0.63	0.84	0.26	0.05	0.57	0.86	0.04
WWU_w	2.40	1.55	2.77	1.94	2.07	1.46	3.04	1.22
$SHGC_w$	0.11	0.17	0.11	0.20	0.11	0.38	0.15	0.22
VLTw	0.18	0.15	0.36	0.23	0.84	0.52	0.60	0.41
ACH	0.51	0.52	0.50	0.65	0.52	1.01	0.53	1.50
OA	264.84	277.93	268.36	280.52	278.24	284.85	208.23	138.12
WWR_s	0.28	0.28	0.31	0.31	0.30	0.31	0.29	0.34
WWR_w	0.62	0.62	0.62	0.62	0.62	0.62	0.62	0.62
OD	1.73	1.51	1.82	1.64	0.53	1.91	1.31	1.87
FD	1.60	1.99	1.55	0.83	1.73	0.01	1.87	1.90

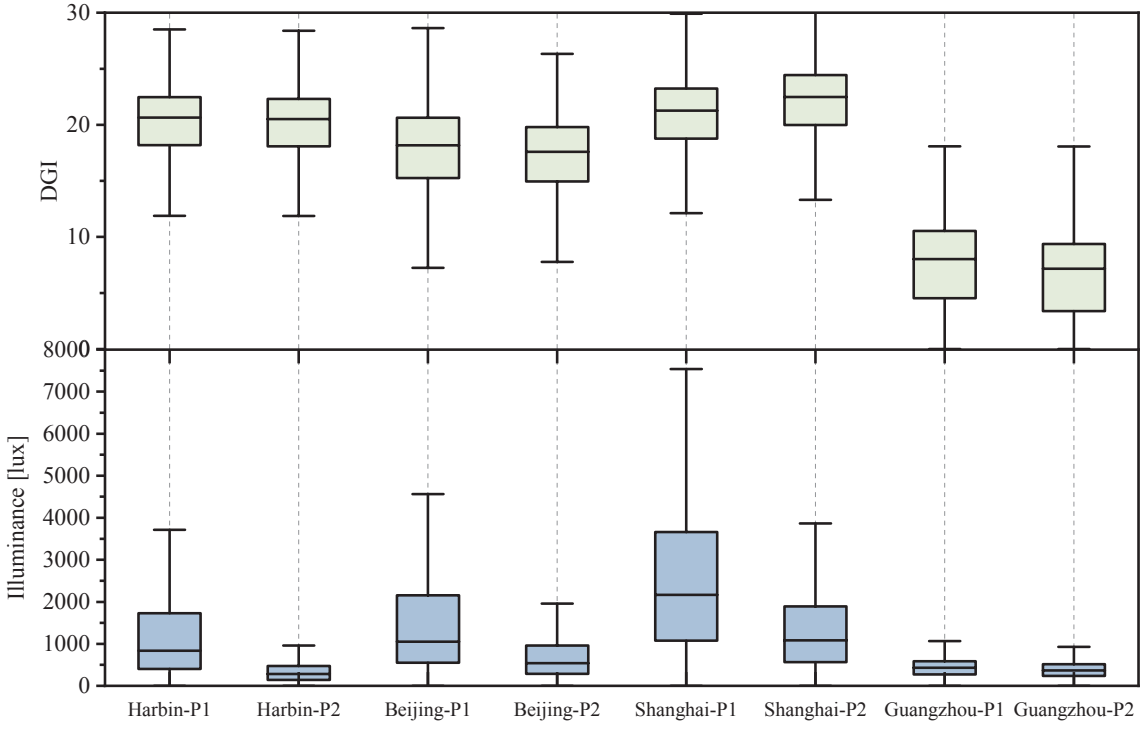

Fig. 12. The indoor DGI and daylighting illuminance of the optimization solution throughout the year.

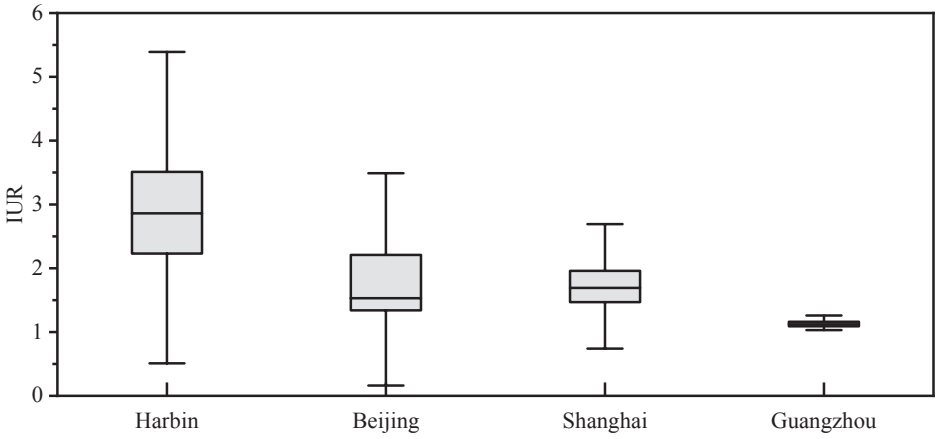

Fig. 13. The illuminance uniformity ratios of the optimization solution throughout the year.

improve the rate of thermal comfort (17.6%), while the other three cities have less than 10% potential, especially Beijing's (3.3%).

This study emphasizes that design scenarios have a significant impact on building design process and can guide architectural engineering design. The results of this study illustrate that the appropriate optimization scheme can be adopted into the building design process considering the achievable degree of adjustment strategies.

CRediT authorship contribution statement

Ran Wang: Conceptualization, Data curation, Formal analysis, Writing - original draft, Writing - review & editing. **Shilei Lu:** Funding acquisition, Methodology, Project administration, Supervision. **Wei Feng:** Validation, Writing - review & editing.

Declaration of Competing Interest

The authors declare that they have no known competing financial interests or personal relationships that could have appeared to influence the work reported in this paper.

Acknowledgment

This research has been supported by the “National Key R&D Program of China” (Grant No. 2016YFC0700100).

References

[1] Yang L, Yan H, Lam JC. Thermal comfort and building energy consumption implications–a review. Appl Energ 2014;115:164–73.
[2] Geyer P, Singaravel S. Component-based machine learning for performance prediction in building design. Appl Energ 2018;228:1439–53.
[3] Chen X, Yang H. Integrated energy performance optimization of a passively designed high-rise residential building in different climatic zones of China. Appl Energ 2018;215:145–58.

[4] Tian W, Heo Y, De Wilde P, Li Z, Yan D, Park CS, et al. A review of uncertainty analysis in building energy assessment. Renew Sustain Energy Rev 2018;93:285–301.
[5] Tian W, Song J, Li Z, de Wilde P. Bootstrap techniques for sensitivity analysis and model selection in building thermal performance analysis. Appl Energ 2014;135:320–8.
[6] Salata F, Ciancio V, Dell'Olmo J, Golasi I, Palusci O, Coppi M. Effects of local conditions on the multi-variable and multi-objective energy optimization of residential buildings using genetic algorithms. Appl Energ 2020;260:114289.
[7] Harkouss F, Fardoun F, Biwole PH. Passive design optimization of low energy buildings in different climates. Energy 2018;165:591–613.
[8] Sun C, Zhang R, Sharples S, Han Y, Zhang H. A longitudinal study of summertime occupant behaviour and thermal comfort in office buildings in northern China. Build Environ 2018;143:404–20.
[9] Jeong B, Jeong J-W, Park J. Occupant behavior regarding the manual control of windows in residential buildings. Energy Build 2016;127:206–16.
[10] Pan S, Xiong Y, Han Y, Zhang X, Xia L, Wei S, et al. A study on influential factors of occupant window-opening behavior in an office building in China. Build Environ 2018;133:41–50.
[11] Rijal HB, Tuohy P, Humphreys MA, Nicol JF, Samuel A, Clarke J. Using results from field surveys to predict the effect of open windows on thermal comfort and energy use in buildings. Energy Build 2007;39:823–36.
[12] Langevin J, Wen J, Gurian PL. Simulating the human-building interaction: Development and validation of an agent-based model of office occupant behaviors. Build Environ 2015;88:27–45.
[13] Fiorentini M, Serale G, Kokogiannakis G, Capozzoli A, Cooper P. Development and evaluation of a comfort-oriented control strategy for thermal management of mixed-mode ventilated buildings. Energy Build 2019;202:109347.
[14] Van Den Wymelenberg K. Patterns of occupant interaction with window blinds: a literature review. Energy Build 2012;51:165–76.
[15] Gunay HB, O'Brien W, Beausoleil-Morrison I, Gilani S. Development and implementation of an adaptive lighting and blinds control algorithm. Build Environ 2017;113:185–99.
[16] Shetabivash H. Investigation of opening position and shape on the natural cross ventilation. Energy Build 2015;93:1–15.
[17] Yu J, Yang C, Tian L. Low-energy envelope design of residential building in hot summer and cold winter zone in China. Energy Build 2008;40:1536–46.
[18] Gou S, Nik VM, Scartezzini J-L, Zhao Q, Li Z. Passive design optimization of newly-built residential buildings in Shanghai for improving indoor thermal comfort while reducing building energy demand. Energy Build 2018;169:484–506.
[19] Liu Z, Liu Y, He B-J, Xu W, Jin G, Zhang X. Application and suitability analysis of the key technologies in nearly zero energy buildings in China. Renew Sustain Energy Rev 2019;101:329–45.
[20] Ramallo-González A, Blight T, Coley D. New optimisation methodology to uncover robust low energy designs that accounts for occupant behaviour or other unknowns. J Build Eng. 2015;2:59–68.
[21] Chen X, Yang H. A multi-stage optimization of passively designed high-rise residential buildings in multiple building operation scenarios. Appl Energ 2017;206:541–57.
[22] Singh R, Lazarus IJ, Kishore V. Uncertainty and sensitivity analyses of energy and visual performances of office building with external venetian blind shading in hot-dry climate. Appl Energ 2016;184:155–70.
[23] Rouleau J, Gosselin L, Blanchet P. Robustness of energy consumption and comfort in high-performance residential building with respect to occupant behavior. Energy. 2019;188:115978.
[24] Wang R, Lu S, Feng W. A three-stage optimization methodology for envelope design of passive house considering energy demand, thermal comfort and cost. Energy 2019;116723.
[25] Prada A, Cappelletti F, Baggio P, Gasparella A. On the effect of material uncertainties in envelope heat transfer simulations. Energy Build 2014;71:53–60.
[26] Chen X, Yang H, Sun K. Developing a meta-model for sensitivity analyses and prediction of building performance for passively designed high-rise residential buildings. Appl Energ 2017;194:422–39.
[27] McKay MD, Beckman RJ, Conover WJ. Comparison of three methods for selecting values of input variables in the analysis of output from a computer code. Technometrics 1979;21:239–45.
[28] Levy S, Steinberg DM. Computer experiments: a review. ASTA-Adv Stat Anal 2010;94:311–24.
[29] Korolija I, Zhang Y, Marjanovic-Halburd L, Hanby VI. Regression models for predicting UK office building energy consumption from heating and cooling demands. Energy Build 2013;59:214–27.
[30] Macdonald I, Strachan P. Practical application of uncertainty analysis. Energy Build 2001;33:219–27.
[31] Breesch H, Janssens A. Performance evaluation of passive cooling in office buildings based on uncertainty and sensitivity analysis. Sol Energy 2010;84:1453–67.
[32] Asadi S, Amiri SS, Mottahedi M. On the development of multi-linear regression analysis to assess energy consumption in the early stages of building design. Energy Build 2014;85:246–55.
[33] Tian W. A review of sensitivity analysis methods in building energy analysis. Renew Sustain Energy Rev 2013;20:411–9.
[34] Mara TA, Tarantola S. Application of global sensitivity analysis of model output to building thermal simulations. Build Simulat: Springer 2008:290–302.
[35] Morris MD. Factorial sampling plans for preliminary computational experiments. Technometrics 1991;33:161–74.
[36] McRae GJ, Tilden JW, Seinfeld JH. Global sensitivity analysis—a computational implementation of the Fourier amplitude sensitivity test (FAST). Comput Chem Eng 1982;6:15–25.
[37] Helton JC, Johnson JD, Sallaberry CJ, Storlie CB. Survey of sampling-based methods for uncertainty and sensitivity analysis. Reliab Eng Syst Safe 2006;91:1175–209.
[38] Prada A, Gasparella A, Baggio P. On the performance of meta-models in building design optimization. Appl Energ 2018;225:814–26.
[39] Ostergard T, Jensen RL, Maagaard SE. A comparison of six metamodeling techniques applied to building performance simulations. Appl Energ 2018;211:89–103.
[40] Delgarm N, Sajadi B, Delgarm S, Kowsary F. A novel approach for the simulation-based optimization of the buildings energy consumption using NSGA-II: Case study in Iran. Energy Build 2016;127:552–60.
[41] Machairas V, Tsangrassoulis A, Axarli K. Algorithms for optimization of building design: a review. Renew Sustain Energy Rev 2014;31:101–12.
[42] Nguyen A-T, Reiter S, Rigo P. A review on simulation-based optimization methods applied to building performance analysis. Appl Energ 2014;113:1043–58.
[43] Shi X, Tian Z, Chen W, Si B, Jin X. A review on building energy efficient design optimization rom the perspective of architects. Renew Sustain Energy Rev 2016;65:872–84.
[44] Pilechiha P, Mahdavinejad M, Rahimian FP, Carnemolla P, Seyedzadeh S. Multi-objective optimisation framework for designing office windows: quality of view, daylight and energy efficiency. Appl Energ 2020;261:114356.
[45] Wate P, Iglesias M, Coors V, Robinson D. Framework for emulation and uncertainty quantification of a stochastic building performance simulator. Appl Energ 2020;258:113759.
[46] Najjar M, Figueiredo K, Hammad AW, Haddad A. Integrated optimization with building information modeling and life cycle assessment for generating energy efficient buildings. Appl Energ 2019;250:1366–82.
[47] Echenagucia TM, Capozzoli A, Cascone Y, Sassone M. The early design stage of a building envelope: multi-objective search through heating, cooling and lighting energy performance analysis. Appl Energ 2015;154:577–91.
[48] Fumo N, Mago P, Luck R. Methodology to estimate building energy consumption using EnergyPlus Benchmark Models. Energy Build 2010;42:2331–7.
[49] Singh R, Lazarus IJ, Kishore V. Effect of internal woven roller shade and glazing on the energy and daylighting performances of an office building in the cold climate of Shillong. Appl Energ 2015;159:317–33.
[50] Ascione F, Bianco N, Mauro GM, Vanoli GP. A new comprehensive framework for the multi-objective optimization of building energy design: harlequin. Appl Energ 2019;241:331–61.
[51] Chen Y, Tong Z, Wu W, Samuelson H, Malkawi A, Norford L. Achieving natural ventilation potential in practice: control schemes and levels of automation. Appl Energ 2019;235:1141–52.
[52] Perez R, Ineichen P, Seals R, Michalsky J, Stewart R. Modeling daylight availability and irradiance components from direct and global irradiance. Sol Energy 1990;44:271–89.
[53] Konis K. A novel circadian daylight metric for building design and evaluation. Build Environ 2017;113:22–38.
[54] Sorgato MJ, Melo AP, Lamberts R. The effect of window opening ventilation control on residential building energy consumption. Energy Build 2016;133:1–13.
[55] Atzeri AM, Cappelletti F, Tzempelikos A, Gasparella A. Comfort metrics for an integrated evaluation of buildings performance. Energy Build 2016;127:411–24.
[56] Chi DA, Moreno D, Navarro J. Correlating daylight availability metric with lighting, heating and cooling energy consumptions. Build Environ 2018;132:170–80.
[57] Piccolo A, Simone F. Effect of switchable glazing on discomfort glare from windows. Build Environ 2009;44:1171–80.
[58] Suk JY, Schiler M, Kensek K. Investigation of existing discomfort glare indices using human subject study data. Build Environ 2017;113:121–30.
[59] Guideline A. Guideline 14-2002, Measurement of Energy and Demand Savings. American Society of Heating, Ventilating, Air Conditioning Engineers, Atlanta, Georgia; 2002.
[60] Chen X, Huang J, Yang H, Peng J. Approaching low-energy high-rise building by integrating passive architectural design with photovoltaic application. J Clean Prod 2019;220:313–30.
[61] Fernández-Agüera J, Domínguez-Amarillo S, Sendra JJ, Suárez R. An approach to modelling envelope airtightness in multi-family social housing in Mediterranean Europe based on the situation in Spain. Energy Build 2016;128:236–53.
[62] Gueymard C. Spectral effects on the transmittance, solar heat gain, and performance rating of glazing systems. Sol Energy 2009;83:940–53.
[63] Wang R, Lu S, Li Q. Multi-criteria comprehensive study on predictive algorithm of hourly heating energy consumption for residential buildings. Sustain Cities Soc 2019;49:101623.
[64] Ma J, Cheng JC. Identification of the numerical patterns behind the leading counties in the US local green building markets using data mining. J Clean Prod 2017;151:406–18.
[65] Guideline A. Guideline 14-2002, Measurement of Energy and Demand Savings. American Society of Heating, Ventilating, Air Conditioning Engineers, Atlanta, Georgia; 2002.
[66] MOHURD. GB50176-93, Thermal design code for civil building. Beijing: China Planning Press; 1993.
[67] Ochoa CE, Aries MB, van Loenen EJ, Hensen JL. Considerations on design optimization criteria for windows providing low energy consumption and high visual comfort. Appl Energ 2012;95:238–45.